Thermal, Mechanical and Shape Memory Properties of Nano-rubber Toughened Epoxy-based Shape Memory Nanocomposites

Hong-Qiu Wei[1], Ye Chen[3], Tao Zhang[4], Liwu Liu[2], Jinliang Qiao[5], Yanju Liu[2*], Jinsong Leng[1]

[1] Center for Composite Materials and Structures, Harbin Institute of Technology (HIT), Harbin 150080, People's Republic of China

[2] Department of Astronautical Science and Mechanics, Harbin Institute of Technology (HIT), Harbin 150080, People's Republic of China

[3] Department of Materials Science and Engineering, Harbin Institute of Technology (HIT) at Weihai, Weihai 264209, People's Republic of China

[4] School of Mechanical and Automotive Engineering, Kingston University, London, SW15 3DW, UK

[5] SINOPEC, Beijing Research Institute of Chemical Industry, Beijing, 100013, People's Republic of China

* Correspondence to: Yanju Liu (Email address: yj_liu@hit.edu.cn)

Abstract

Epoxy-based shape memory polymer (ESMP) is a kind of the most promising engineering smart polymers. However, the inherent brittleness limits its application. The existing modification approaches are either based on complicated chemical reactions or at the cost of thermal properties of ESMP. In this study, a simple approach is made to the fabrication of ESMP aiming to improve its overall properties by introducing cross-linked carboxylic nitrile/butadiene nano-rubber (CNBNR) into ESMP network. The results show that the toughness of CNBNR/ESMP nanocomposites greatly improved at both room temperature and T_g in comparison with pure ESMP. Meanwhile, the increase of toughness has no sacrifice of other macroscopic properties. CNBNR/ESMP nanocomposites present improved thermal properties

with glass transition temperature (T_g) in a stable range around 100 ºC, enhanced thermal stabilities, and superior shape memory performance in terms of shape fixing ratio, shape recovery ratio, shape recovery time and repeatability of shape memory cycles. The combined property improvements and the simplicity in manufacture process demonstrate that CNBNR/ESMP nanocomposites are desirable candidates for large-scale application in engineering field as smart structural materials.

Keywords: A. Smart materials, Nano composites; B. Mechanical properties, Thermal properties, Thermomechanical properties

1. Introduction

Shape memory polymers (SMPs) as a class of smart materials are capable of returning to its initial shape from a temporary shape when they are actuated by heat, light, electrical or magnetic fields, moisture, and PH value, etc.[1-6] These smart characteristics enable SMPs potentially to be applied in the areas ranging from deployable aerospace structures to biomedical devices.[7-12] SMPs are generally divided into either thermoplastic or thermoset classes according to the chemical structures. The networks of thermoset SMPs are based on covalently cross-linking points, while those of thermoplastic SMPs are usually consisted of physically cross-linking points.[1,10,13,14] Compared with thermoplastic SMPs, thermoset SMPs always present high reliability and superior shape memory behavior because of their stable covalently cross-linking networks.[15,16] Owing to such unique features, thermoset SMPs have been investigated extensively in recent years.

Epoxy-based SMPs (ESMPs) are one of the most important thermoset SMPs. Except for the general capabilities of thermoset SMPs, ESMPs also provide their own attractive properties, including adjustable and high glass transition temperature (T_g>80 ºC), excellent thermal

performance, high modulus and fracture strength, rapid responsive speed, chemical durability, and easy processing, etc.[17-22] These characteristics make ESMPs extremely acceptable to be applied as engineering smart and structural materials. However, pristine ESMPs suffer from inherent brittleness caused by the relatively high cross-linking structures.[23-26] Such drawbacks induce ESMPs sensitive to fatigue and cracks, which severely hinders their way for practical applications.[25] To overcome this challenge, extensive researches to improve the toughness of ESMPs have been carried out worldwide.[25,27-30] For examples, Hartwig et al. prepared ESMPs with partially crystal structures by cationic polymerization with poly (ω-pentadecalactone) (PPDL). Such epoxy/PPDL composite showed good shape-memory cycle stability and enhanced strength and toughness.[27] Huang et al. fabricated a novel ESMP by introducing oxyethylene groups to diglycidyl ether of 9,9-bis (4-hydroxyphenyl) fluorine (DGEBF). The cured 9,9-bis [4-(2-hydroxyethoxy) phenyl] fluorine/4,4'-diamin-odiphenylsulfone (DGEBEF/DDS) polymeric network exhibited superior low water uptake, mechanical properties and thermal stability.[28] Xie, et al. recently reported a kind of ESMP with strain at break of 111% above T_g and 212% at T_g, respectively.[25] They greatly improved the toughness of ESMPs at high temperature.

The above mentioned researches have significantly paved the way for improving the toughness of ESMPs. However, some of the modification methods rely on complicated chemical reactions which restrict large-scale applications of ESMPs, while others either sacrifice their thermal capabilities or mechanical properties at room temperature. It is still urgently needed to further enhance the overall performance and simplify the fabrication methods for ESMPs to enable their large-scale applications as smart structural materials in engineering and other necessary areas. To achieve this, simple and effective composite approaches always are used for the development of

ESMPs. Previous composite strategies generally focused on carbon nanotubes, carbon black, carbon fibers, iron oxide, and silicon carbide, etc.[18,31-36] These fillers greatly improved the thermal properties and mechanical strength of ESMPs. However, the toughness of such stiff fillers reinforced ESMP composites declined seriously. Moreover, it is quite difficult to use them as composite matrix for smart structures.

Cross-lined carboxylic nitrile/butadiene nano-rubber (CNBNR) powder is well-known for toughening epoxy without cost of their heat resistance.[37,38] Meanwhile, CNBNR is easy to be uniformly dispersed in epoxy resins and preserve the characteristic of epoxy for composite matrix.[39,40] Therefore, such kind of elastomeric nanoparticles may be one of the best choices of fillers for ESMP-based composites to achieve excellent comprehensive performances. Based on these advantages, in this study, CNBNR was introduced into ESMP network for improving the toughness and maintain other macroscopic properties of such smart material to broaden their engineering applications. A systematic research is constructed on CNBNR/ESMP nanocomposites. The macroscopic capabilities, including thermal properties, thermal stabilities, and mechanical properties are investigated in detail. The potential mechanism of CNBNR for improving the overall properties of CNBNR/ESMP nanocomposites are discussed. We achieve the optimized content of CNBNR for the excellent overall properties, and the shape memory performance of nano-rubber toughed materials are first systematically investigated.

Materials and Methods

2.1 Materials

The epoxy-based shape memory polymer (ESMP) was prepared according to our previous studies, which was a kind of thermoset cross-linking network containing three ingredients-epoxy resin, hardener and accelerator.[30] Cross-linked carboxylic nitrile/butadiene nano-rubber powder

(CNBNR, Narpow VP-501 particle size distribution: 50-100 nm, T_g: -29.1 ºC, acrylonitrile content: 26 *wt.*%), was supplied by Beijing Research Institute of Chemical Industry, China. To remove the moisture, CNBNR was dried in an oven at 50 ºC for 24 h under vacuum before mixing.

2.2 Methods

2.2.1 Sample preparation

Firstly, a masterbatch was prepared. 20 phr (per hundred parts epoxy resin) CNBNR was added into a baker containing 100 phr epoxy resin and premixed by manual stirring for 10 min. The obtained mixture was transferred to ARE 500 planetary centrifugal mixer for speed mixing at 300 rpm for 3 min, 500 rpm for 2 min and 1000 rpm for 1 min. To achieve homogeneous masterbatch, the above blend was further dispersed by three-roll mill for 6 times with gradually reduced the gap between rollers (from 30 μm to 5 μm). The ready masterbatch was then divided into four parts with equal weight. Different amounts of epoxy resin (75, 25, 8.3, 0 g) and hardener (80, 40, 26.7, 20 g) were added into each part, respectively, to prepare 5, 10, 15, and 20 phr CNBNR/ESMP nanocomposites. The mixing process was proceeded by continuously mechanical stirring with speed gradually increasing from 300 rpm to 1000 rpm at 80 ºC. After 45 min, accelerator was given with the weight ratio of accelerator/(epoxy resin+ hardener) = 1/50, and mixed for another 10 min at 1000 rpm. Such blend was degassed in a vacuum oven at 80 ºC for 15 min to remove bubbles. Then, it was put into preheated glass molds with different thickness and cured at 80 ºC for 2 h, 100 ºC for 3 h, and 150 ºC for another 5 h. The CNBNR/ESMP nanocomposites could be achieved by cooling down to room temperature. For comparison, pure ESMP was fabricated by directly mixing epoxy resin, hardener and accelerator by mechanical stirring at 300 rpm. The curing condition of pure ESMP was set the same with

CNBNR/ESMP nanocomposites. The nomenclature and the composition of the prepared materials are given in Table 1.

2.2.2 Characterizations

Thermal Analysis. Differential Scanning Calorimetry (DSC: DSC/700/1410, Mettler-Toledo) was used to study the phase transition behaviors. The temperature ranged in 25~200 ºC with a rate of 5 ºC /min under nitrogen atmosphere. The thermal stabilities were tested by Thermogravimetric Analysis (TGA: TGA/DSC1 SF1942, Mettler-Toledo) under nitrogen atmosphere with the temperature changing from 25 ºC to 600 ºC at 10 ºC /min. The chemical structures were conducted using a Fourier Transform Infrared (FTIR: Spectrum One, PerkinElmer) spectrometer by dispersing powder sample in a KBr pellet. The test was undertaken in a spectral range of 4000–370 cm^{-1} and a resolution of 4 cm^{-1}.

Static Mechanical Analysis. The static mechanical properties at room temperature (25±2 ºC) and 100 ºC were characterized by a universal material testing machine (Z050, Zwick/Roell) with a thermal chamber under tensional mode. Dog-bone shaped specimens (ASTM D638, Type IV) were cut off from the prepared plates by a laser cutting machine. A crosshead speed of 5 mm/min was utilized for testes at both room temperature and at 100 ºC. The fractured surfaces were observed by Scanning Electron Microscopy (SEM: VEGA3SB, Tescan) after sputter-coating with gold.

Shape memory behavior. Dynamic Mechanical Analysis (DMA: Q800, TA Instruments) under single-cantilever mode was carried out to evaluate the thermal-mechanical properties. The temperature ranged from 25 ºC to 150 ºC at a rate of 5 ºC/min. A frequency of 1Hz was employed during the whole test. Sample dimension is 35×13×3 mm^3. A bending-recovery test was carried out to qualitatively investigate the shape memory behavior. A rectangular specimen

with dimension of 30×5×1 mm^3 was defined as original shape. First, it was heated to T_g and bended into a "U"-like shape after it became flexible. Then, temporary shape was achieved by cooling down the deformed shape to room temperature under external force. The shape recovery phenomenon was monitored by imaging process when reheating the deformed sample to T_g. The shape recovery time and the shape recovery angle as a function of time were obtained from the recorded images. Shape memory cycle (SMC) proceeded on DMA (Q800, TA Instruments) was utilized to characterize the shape memory behavior quantitatively. The test was performed under tensional film fixture and a preload of 0.01N was imposed (30×4×1 mm^3) to protect specimen from slide. The procedures for the SMC include (Figure S1): 1) Heat the sample to T_g for deformation. 2) Isothermally stretch the soft sample to a certain strain with a constant stress. 3) Cool down the deformed sample to room temperature under the same load to maintain the temporary shape. 4) Elevate temperature to T_g to induce the active shape recovery. Shape fixed ratio (R_f) and shape recovery ratio (R_r) were obtained by the following equations[19,41-43]:

$$R_f = \frac{\varepsilon_f}{\varepsilon_{load}} \times 100\% \quad (1)$$

$$R_r = \frac{\varepsilon_f - \varepsilon_{rec}}{\varepsilon_f} \times 100\% \quad (2)$$

where ε_{load} stands for the strain under external stress, ε_f is the strain after unloading, ε_{rec} represents for residual strain after recovering.

3. Results and Discussion

3.1 Thermal properties

Figure 1 shows the thermal analysis results for pure ESMP, CNBNR and CNBNR/ESMP nanocomposites. The typical DSC curves in Figure 1a reflect the thermal transition behavior of the prepared materials. To eliminate the influence of heating history, the secondary heating scan

is used in this analysis. The step in Figure 1b indicates the occurrence of glass transition during heating process. The DSC results qualitatively show that the introduction of CNBNR has no negative effects on T_g. Instead, most T_g of CNBNR/ESMP nanocomposites are slightly higher than that of pure ESMP. Those results agree with previous studies done for the CNBNR toughed commercial epoxy composites. [38,39]

Thermal stabilities of CNBNR/ESMP nanocomposites can be evaluated in Figure 1c-1d. For each sample, only one degradative stage is found (Figure 1c), which is caused by the decomposition of polymeric backbone. Important thermal elements, including T_d (temperature relating to 5% weight loss), char yield, T_{max} (temperature of peak value in DTG curves) are extracted and listed in Table 2. Obviously, the decomposition of all the materials (relating to T_d) starts at above 325 ^{o}C, and most of them are higher than 347 ^{o}C. The major decomposition, judging by T_{max}, occurs at about 380 ^{o}C. These results demonstrate that the fabricated smart nanocomposites could be manipulated safely around their T_g range. Further observation find that CNBNR/ESMP nanocomposites show higher T_d, T_{max} and char yield in comparison with the pure ESMP (except for the sample of 20 phr). It indicates that the thermal stabilities of CNBNR/ESMP nanocomposites are slightly improved by introducing CNBNR to the polymeric network.

From the consequences, it is easy to conclude that CNBNR/ESMP nanocomposites with addition of CNBNR less than 15 phr possessed better thermal capabilities than pure ESMP network. To study the possible reasons, FTIR tests were carried out and the results are shown in Figure 2. It can be obtained from Figure 2a that the improvement of the thermal properties is not caused by chemical reaction between CNBNR and ESMP, since there is no difference in their FTIR characteristic peaks. A close observation from the selected part in Figure 2a finds that the

absorption peaks belonging to hydroxyl group gradually move to a lower frequency as the content of CNBNR increasing (Figure 2b). It indicates the presence of enhanced hydrogen bonding between ESMP and CNBNR, which is the explanation for the increased thermal performance.[37,38] However, sample 20 phr is discovered for a decreased thermal properties and thermal stabilities comparing with pure ESMP. This is because when large amount of low T_g material is added to a system, the part not join the network will not only decrease the interaction between nano-fillers and polymer matrix, but also result in a less cross-linking degree of the material system. In that case, lower T_g and T_d are achieved.

3.3 Static mechanical properties

To investigate the effectiveness of our proposed modification method on static mechanical properties, tensional tests were performed on CNBNR/ESMP nanocomposites at room temperature. Corresponding data are plotted in Figure 3a. The typical stress-strain curves vary from linearity to non-linearity gradually, indicating the mechanical behaviors of the prepared materials changing from brittle to ductile when the content of CNBNR is increased. Such phenomenon is also verified by the SEM images shown in Figure 4. The fractured surface of pure ESMP is extremely smooth, which reveals the highly brittle breakage (Figure 4a). However, the fractured cross-section in Figure 4b-4e become increasingly rough. Varied cracks propagations, plastic zone and shear flow become more and more visible and the amounts of them increases markedly as the content of CNBNR changing from 5 phr to 20 phr. It clearly indicates the fractured mode of the materials turns into ductile breakage.[18,44] In Figure 3b, an increase of *elongation at break* (ε_b) in the range of 49.5-736.4% can be seen by changing the content of CNBNR from 5 phr to 20 phr. However, only a slight drop of *Young's Modulus (E)* (5.6%-16.4%) is found as the CNBNR content varying from 5 phr to 20 phr, indicating the

remarkable improvement of ε_b has no dramatically negative effect on E. Meanwhile, *maximum strength* (σ_m) improves by 29.2% when 10 phr CNBNR is used, although it presents a small decline after first increase. These results suggest that the introduction of CNBNR can greatly improves the ductility of CNBNR/ESMP nanocomposites and can maintain or slightly increase the strength at room temperature.

For ESMPs, it is equally important to investigate the static mechanical properties at temperature above T_g, because ε_b at rubbery state is an important parameter for their deforming performance. In Figure 3c, the typical stress-strain curves demonstrate that the ductility at rubbery state boosts by the addition of CNBNR. ε_b values are improved from 22.1% for the pure ESMP to 44.7% for sample 20 phr CNBNR. It demonstrated the improvement of deformation capabilities of CNBNR/ESMP nanocomposites. Large deformation can be achieved at rubbery state without the breakage of the specimen, and this will be able to increase the safety and applications of ESMPs.

The area of strain-stress curve is always used for evaluating the toughness of the materials. From Figure 3d, it can be observed that both the toughness of CNBNR/ESMP nanocomposites at room temperature (KIc_{rt}) and 100 ^{o}C ($KIc_{100\ ^{o}C}$) greatly improved in comparison with pure ESMP. Such results indicate the effectiveness of CNBNR for toughening ESMP.

The enhancement of mechanical properties at both room temperature and high temperature are due to the introduction of flexible nano-fillers to the polymeric network. The ductile feature of CNBNR contributes to the high toughness of the materials, while the large surface energy caused by their nano-scale sizes and enhanced hydrogen bonding between CNBNR and ESMP are key driving elements for the high strength and modulus.[38,39] In general, CNBNR/ESMP nanocomposites show significantly enhanced mechanical properties.

3.3 Shape memory properties

Thermal-mechanical property was firstly studied as it has close relationship with shape memory behavior. Figure 5a shows that all the tested samples present a glassy platform at low temperature and follow by a sudden drop to the rubbery platform at high temperature. Such transformation reveals the occurrence of glass-rubber transition during heating process. Importantly, the changes of storage modulus between glassy state and rubbery state reach two orders of magnitude. It is the necessary pre-condition for shape memory function.[30] Peak value of loss factor is important reference for T_g. From Figure 5b and Table 2, it can be found that T_g values vary in a narrow range around 100 ^{o}C. Moreover, the variation trend of T_g values obtained from DMA is similar to those obtained from DSC (Figure 2a). The increased T_g of CNBNR/ESMP nanocomposites in comparison of pure ESMP is attributed to the enhanced hydrogen bonding as we illustrated before. However, still no higher T_g is observed for sample 20 phr. The underlying explanation can be found from SEM images in Figure 4. Different from others, some holes appear on the fractured surface of the sample 20 phr (Figure 4e), which can be clearly seen in Figure 4f. The presence of that indicates the nano-fillers aggregate into microscale particles, leading to less interfacial adhesion between CNBNR and ESMP. In that case, CNBNR acts as normal rubber.[39] Although it is still effective for improving toughness, no enhancement on thermal properties can be found.[38]

DMA results reveal that all CNBNR/ESMP samples display glass-rubber transitions, dramatic changes of storage modulus during heating process and final flat rubbery platforms. It indicates that all CNBNR/ESMP specimens are supposed to possess shape memory functions.[25] Herein, sample 15 phr is chosen for deep investigation of shape memory behavior based on its relatively excellent thermal and mechanical properties. A bending-recovery experiment was conducted firstly to qualitatively characterize the shape memory behavior. The corresponding results are

shown in Figure 6a-6b. The temporary “U”-like shape unfolds to the initial “-”-like shape with a fairly fast responsive speed. The shape recovery angle increases rapidly with time, and the entire shape recovery process happens in merely 25 s with nearly 100% shape recovery. Such consequences visually demonstrate the excellent shape memory performance of CNBNR/ESMP nanocomposite. SMC test was carried out on DMA to quantitatively analyze the shape memory function for the sample of 15 phr. To eliminate the effect of stress history, a secondary SMC is presented in Figure 6c for analyzing. According to Eq. 1 and Eq. 2, the calculated R_f and R_r are up to 96.3% and 97.6%, respectively, which implies the high shape fixing and recovery performance of CNBNR/ESMP nanocomposite.

It can be concluded from both quantitative and qualitative characterizations that CNBNR/ESMP nanocomposites present excellent shape memory performance. Such results are owing to the introduction of CNBNR to the ESMP network. As reported, shape memory behavior of polymer is based on their two-phase structures. One is soft domain that function to the shape deformation, the other is hard domain which is responsible for memorizing the original shape and shape fixation [2, 4, 13]. The introduction of elastic CNBNR nano-fillers indicates the increase of soft domains in ESMP network. More movable molecular segments contribute the easy deformation and fast recovery of CNBNR/ESMP nanocomposite. Meanwhile, the enhanced hydrogen bonds between CNBNR and ESMP construct more hard domains in the network, which enables high R_f and R_r for CNBNR/ESMP nanocomposite.

Ten SMCs were further carried out to verify the repeatability of shape memory behavior. In Figure 6d, it can be seen that these cycles present reproducibility and consistency with high R_f and R_r. Importantly, no damages appear even after ten testing cycles. This suggests that the shape memory behavior of the CNBNR/ESMP nanocomposite is highly repeatable with superior

fatigue resistance due to the high toughness at both room temperature and 100 ºC. The near perfect shape memory behavior enable CNBNR/ESMP desirable for engineering smart application.

4. Conclusions

A series of thermosetting shape memory nanocomposites of CNBNR/ESMP were constructed successfully, and their overall properties were investigated systematically. The thermal properties of the prepared nanocomposites were slightly improved in comparison to pure ESMP. CNBNR/ESMP nanocomposites showed T_g values varying in a narrow range around 100 ºC (according to DMA test), high T_d and T_{max} up to 350 ºC and 380 ºC, respectively. It was also found that CNBNR/ESMP nanocomposites provided greatly enhanced ductility and strength at both room temperature and above T_g without excessive decrease of modulus. FTIR and SEM analysis indicated that enhanced hydrogen bonding and dispersion status of the nano-fillers were two controlled elements for the improvement of macro-scope properties of CNBNR/ESMP nanocomposites. Moreover, CNBNR/ESMP nanocomposite was demonstrated to possess near perfect and highly repeatable shape memory behavior. This research provides a feasible way for fabrication ESMP-based nanocomposite with improved toughness, meanwhile, without sacrifice of other properties, especially thermal properties and Young's Modulus. Such combined improvement of properties enable their large-scale applications in engineering fields.

Acknowledgments

This work is supported by the National Natural Science Foundation of China (Grant Nos 11225211), for which we are very grateful.

References

1. Zhao, Q.; Qi, H. J.; Xie, T., Prog. Polym. Sci. 2015, 49-50, 79-120.
2. Leng, J. S.; Lan, X.; Liu, Y. J.; Du, S. Y., Prog. Mater. Sci. 2011, 56, 1077-1135.

3. Huang, W. M.; Yang, B.; Zhao, Y.; Ding, Z., J. Mater. Chem. 2010, 20, 3367-3381.
4. Liu, C.; Qin, H.; Mather, P. T., J. Mater. Chem. 2007, 17, 1543-1558.
5. Lendlein, A.; Jiang, H. Y.; Junger, O.; Langer, R., Nature 2005, 434, 879-882.
6. Glock, S.; Canal, L. P.; Grize, C. M.; Michaud, V., Compos. Sci. Technol. 2015, 114, 110-118.
7. Lendlein, A.; Langer, R., Science 2002, 296, 1673-1676.
8. Liu, Y. J.; Du, H. Y.; Liu, L. W.; Leng, J. S., Smart Mater. Struct. 2014, 23, 023001.
9. Zarek, M.; Layani, M.; Cooperstein, I.; Sachyani, E.; Cohn, D.; Magdassi, S., Adv. Mater. 2016, 28, 4449-4454.
10. Hu, J. L.; Zhu, Y.; Huang, H. H.; Lu, J., Prog. Polym. Sci. 2012, 37, 1720-1763.
11. Wang, Y. K.; Tian, W. C.; Xie, J. Q.; Liu, Y., Micromachines 2016, 7, 145.
12. Hu, J. L.; Meng, H. P.; Li, G. Q.; Ibekwe, S. I., Smart Mater. Struct. 2012, 21, 053001.
13. Meng, H.; Li, G. Q., Polymer 2013, 54, 2199-2221.
14. Ratna, D.; Karger-Kocsis, J., J. Mater. Sci. 2008, 43, 254-269.
15. Dong, Y. B.; Ni, Q. Q.; Fu, Y. Q., Composites, Part A 2015, 72, 1-10.
16. Yu, K.; McClung, A. J. W.; Tandon, G. P.; Baur, J. W.; Qi, H. J., Mech. Time-Depend. Mater. 2014, 18, 453-474.
17. Kumar, K. S. S.; Biju, R.; Nair, C. P. R., React. Funct. Polym. 2013, 73, 421-430.
18. Liu, Y. Y.; Zhao, J.; Zhao, L. Y.; Li, W. W.; Zhang, H.; Yu, X.; Zhang, Z., ACS Appl. Mater. Interfaces 2016, 8, 311-320.
19. Rousseau, I. A.; Xie, T., J. Mater. Chem. 2010, 20, 3431-3441.
20. Wei, K.; Ma, B.; Liu, Y.; Wang, H. N.; Li, N., J. Mater. Res. 2015, 30, 2179-2187.
21. Zou, Q.; Ba, L. H.; Tan, X. C.; Tu, M. J.; Cheng, J.; Zhang, J. Y., J. Mater. Sci. 2016, 51, 10596-10607.
22. Wei, H. Q.; Yao, Y. T.; Liu, Y. J.; Leng, J. S., Composites, Part B 2015, 83, 7-13.
23. Fan, M. J.; Li, X. Y.; Zhang, J. Y.; Cheng, J., J. Therm. Anal. Calorim. 2015, 119, 537-546.
24. Zhang, C. H.; Wei, H. G.; Liu, Y. Y.; Tan, H. F.; Guo, Z. H., High Perform. Polym. 2012, 24, 702-709.
25. Zheng, N.; Fang, G. Q.; Cao, Z. L.; Zhao, Q.; Xie, T., Polym. Chem. 2015, 6, 3046-3053.
26. Liu, Y. Y.; Han, C. M.; Tan, H. F.; Du, X. W., Mater. Sci. Eng., A 2010, 527, 2510-2514.

27. Arnebold, A.; Hartwig, A., Polymer 2016, 83, 40-49.
28. Wu, X.; Yang, X.; Zhang, Y.; Huang, W., J. Mater. Sci. 2016, 51, 3231-3240.
29. Leonardi, A. B.; Fasce, L. A.; Zucchi, I. A.; Hoppe, C. E.; Soule, E. R.; Perez, C. J.; Williams, R. J. J., Eur. Polym. J. 2011, 47, 362-369.
30. Leng, J. S.; Wu, X. L.; Liu, Y. J., Smart Mater. Struct. 2009, 18, 095031.
31. Chen, L.; Li, W. B.; Liu, Y. J.; Leng, J. S., Composites, Part B 2016, 91, 75-82.
32. Dong, Y. B.; Ni, Q. Q., Polym. Compos. 2015, 36, 1712-1720.
33. Zhang, Z. Y.; Zhang, H.; Shou, J. Q.; Sun, Y. Y.; Liu, Y. Q., New Carbon Mater. 2015, 30, 404-411.
34. Dong, Y. B.; Ding, J.; Wang, J.; Fu, X.; Hu, H. M.; Li, S.; Yang, H. B.; Xu, C. S.; Du, M. L.; Fu, Y. Q., Compos. Sci. Technol. 2013, 76, 8-13.
35. Ding, J.; Zhu, Y. F.; Fu, Y. Q., Polym. Compos. 2014, 35, 412-417.
36. Wong, T. T.; Lau, K. T.; Tam, W. Y.; Leng, J. S.; Wang, W. X.; Li, W. B.; Wei, H. Q., Compos. Struct. 2015, 132, 1056-1064.
37. Qi, G. C.; Zhang, X. H.; Li, B. H.; Song, Z. H.; Qiao, J. L., Polym. Chem. 2011, 2, 1271-1274.
38. Huang, F.; Liu, Y. Q.; Zhang, X. H.; Wei, G. S.; Gao, J. M.; Song, Z. H.; Zhang, M. L.; Qiao, J. L., Macromol. Rapid Commun. 2002, 23, 786-790.
39. Ozdemir, N. G.; Zhang, T.; Aspin, I.; Scarpa, F.; Hadavinia, H.; Song, Y., eXPRESS Polym. Lett. 2016, 10, 394-407.
40. Ozdemir, N. G.; Zhang, T.; Hadavinia, H.; Aspin, I.; Scarpa, F., J. Compos. Mater. 2016, 50, 2633-2645.
41. Xie, T., Nature 2010, 464, 267-270.
42. Dolog, R.; Weiss, R. A., Macromolecules 2013, 46, 7845-7852.
43. Li, X. X.; Zhu, Y. F.; Dong, Y. B.; Liu, M.; Ni, Q. Q.; Fu, Y. Q., J. Nanomater. 2015, 475316.
44. Li, B. H.; Zhang, X. H.; Gao, J. M.; Song, Z. H.; Qi, G. C.; Liu, Y. Q.; Qiao, J. L., J. Nanosci. Nanotechnol. 2010, 10, 5864-5868.

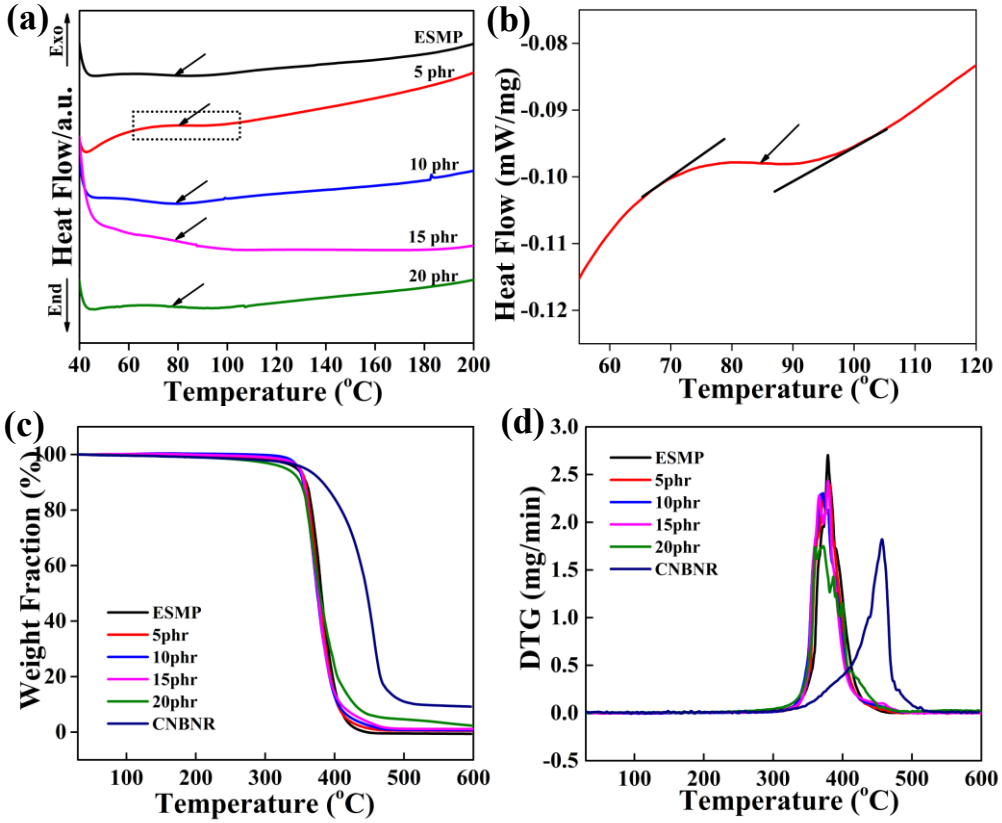

Figure 1. Thermal properties of pure ESMP and CNBNR/ESMP nanocomposite: a. DSC thermo-grams; b. A magnification for selected part in Figure 1a; c. TG curves; d. DTG curves.

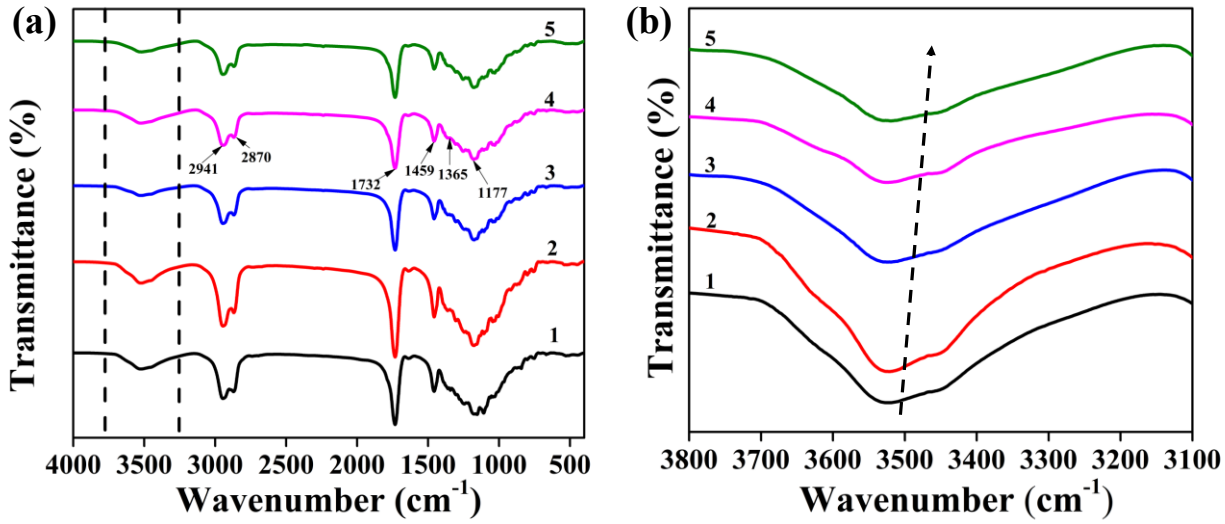

Figure 2. Chemical structure of pure ESMP and CNBNR/ESMP nanocomposites: a. FTIR spectrums; b. The selected area in Figure 3a with high magnification. (1. pure ESMP; 2. 5phr; 3. 10 phr; 4. 15 phr; 5. 20 phr)

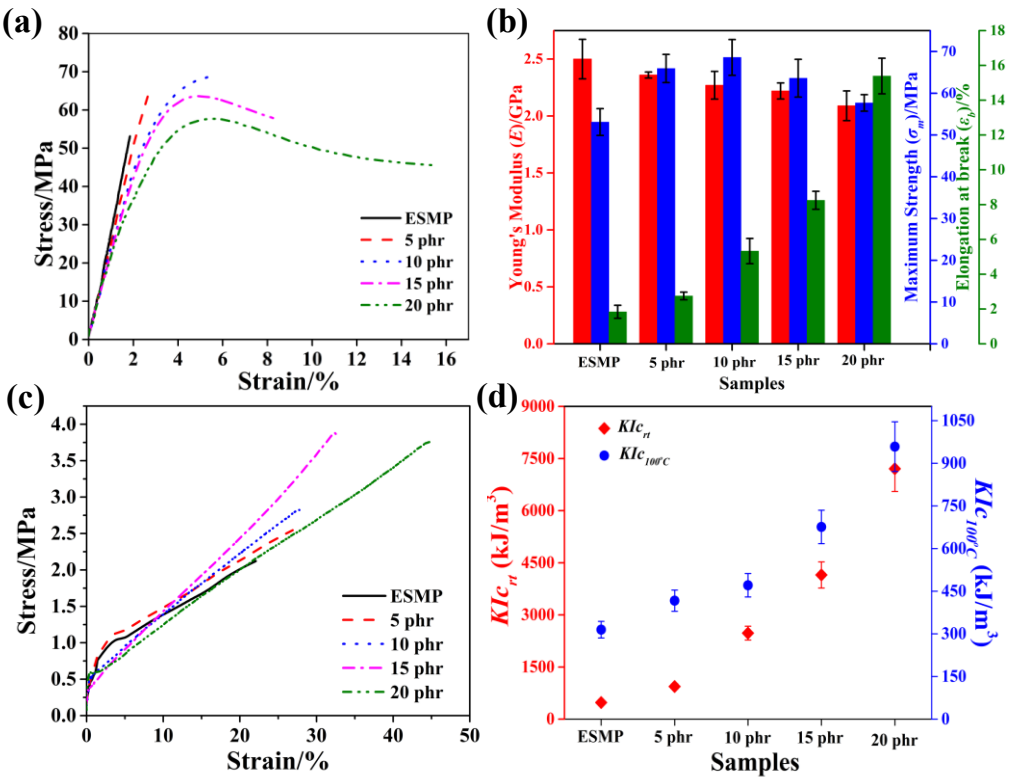

Figure 3. Mechanical properties of pure ESMP and CNBNR/ESMP nanocomposites: a. Typical stress-strain curves at room temperature; b. Results of tensional test at room temperature; c. Typical stress-strain curves at 100 ºC; d. *KIc* at room temperature and 100ºC.

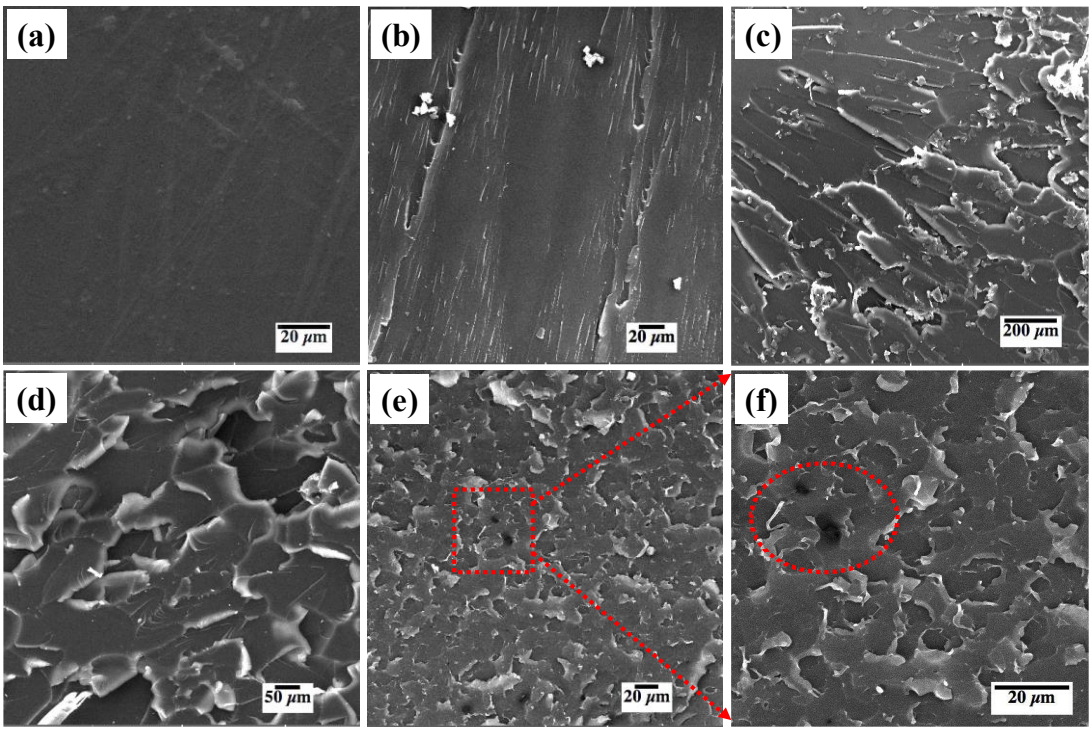

Figure 4. SEM images of tensional fractured cross section of CNBNR/ESMP nanocomposite series: a. Pure ESMP; b. 5 phr; c. 10 phr; d. 15 phr; e. 20 phr; f. A magnification for selected part in Figure 4e.

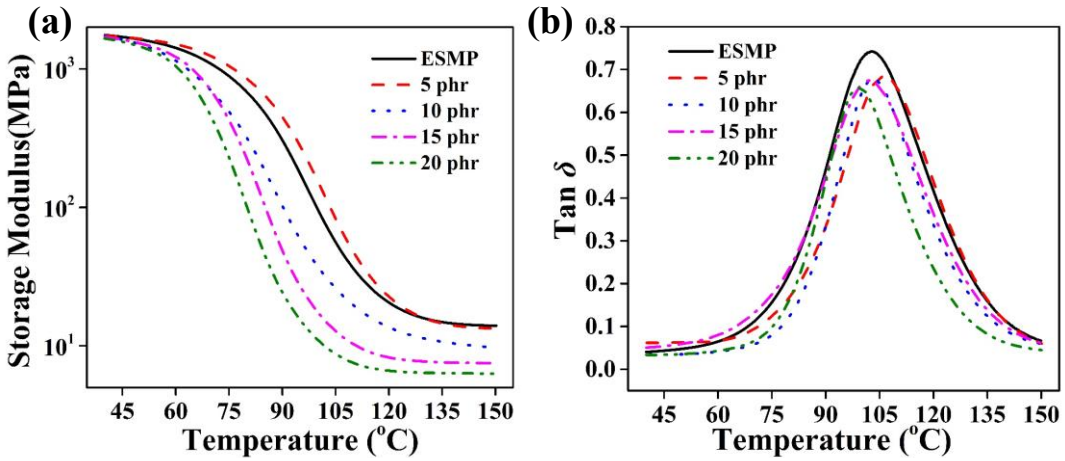

Figure 5. DMA results of pure ESMP and CNBNR/ESMP nanocomposites: a. Storage modulus and b. Tan δ as a function of temperature.

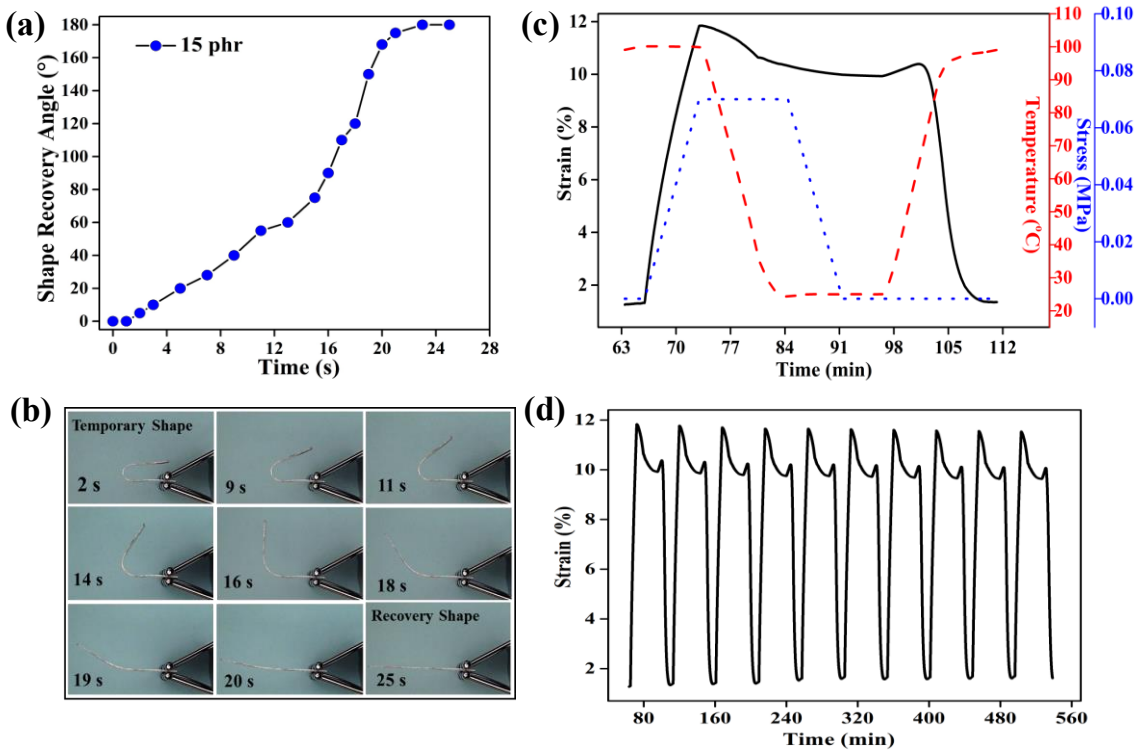

Figure 6. Characterization of shape memory behavior of sample 15 phr: a. Shape recovery as a function of time; b. Visual demonstration of shape memory behavior at 100 ºC; c. The secondary SMC proceeded on DMA; d. Ten SMCs performed on DMA.

Table 1. Compositions of CNBNR/ESMP nanocomposites

Ingredient / Sample	Epoxy resin (g)	Hardener (g)	Accelerator (g)	CNBNR (g)
ESMP	25	20	0.9	0
5 phr	100	80	3.6	5
10 phr	50	40	1.8	5
15 phr	33.3	26.7	1.2	5
20 phr	25	20	0.9	5

Table 2. Thermal Properties of pure ESMP, CNBNR and CNBNR/ESMP nanocomposites

Sample Name	TGA			DMA
	T_d (°C)	T_{max} (°C)	Char yield (%)	T_g (°C)
ESMP	344.9	378.6	0	102.9
5 phr	349.6	380.3	0.5	106.5
10 phr	347.8	378.9	0.7	103.5
15 phr	348.9	378.7	1.1	101.2
20 phr	329.7	375.0	2.3	99.5
CNBNR	357.3	457.1	9.2	-

Graphical Abstract